ISSN 1027-5495. Functional Materials, 27, No.4 (2020), p. 681-686.
doi:https://doi.org/10.15407/fm27.04.681 © 2020 — STC "Institute for Single Crystals"

Solution growth and characterization of high-quality organic 4-*N*,*N*′-dimethylamino-*N*-methyl-4-stilbazolium tosylate crystals

***G.N.Babenko*[1], *A.P.Voronov*[1], *E.F.Dolzhenkova*[1], *V.S.Zadorozhny*[1], *I.M.Pritula*[1], *R.Galbadrakh*[2], *L.Enkhtor*[2]**

[1]Institute for Single Crystals, STC "Institute for Single Crystals", National Academy of Sciences of Ukraine, 60 Lenin Ave., 61001 Kharkiv, Ukraine
[2]Department of Physics, School of Arts and Sciences, National University of Mongolia, 14201 Ikh Surguuliin gudamj1, Sukhbaatar district, Ulaanbaatar, Mongolia

Received June 30, 2020

High-quality 4-*N*,*N*′-dimethylamino-*N*-methyl-4-stilbazolium tosylate crystals has been grown onto a seed from supersaturated methanol solution by controlled temperature lowering method. XRD studies confirm structural perfection of the grown crystals. The functional groups of DAST were identified by FTIR studies. The average values of microhardness obtained on the surface and on the cleaved facet of the grown crystals are different and amount 28.1 and 32.6 kgf/mm^2, respectively. There is established a correlation between the values of microhardness and the character of distribution of dislocations in the DAST crystals.
Keywords: organic crystals, structural perfection, microhardness, dislocation density.

Вирощування з розчину та характеризація високоякісних органічних кристалів тозилату 4-*N*,*N*′-диметиламіно-*N*-метил-4-стілбазолу. *Г.М.Бабенко, О.П.Воронов, О.Ф.Долженкова, В.С.Задорожній, І.М.Притула, Р.Галбадрах, Л.Енхтор*

Високоякісні кристали тозилату 4-*N*,*N*′-диметиламіно-*N*-метил-4-стильбазолу вирощено на затравці з перенасиченого розчину метанолу методом контрольованого зниження температури. Високу структурну досконалість вирощених кристалів підтверджено методом рентгенофазового аналізу. Наявність функціональних груп, що відповідають кристалу DAST, ідентифіковано за допомогою інфрачервоної спектроскопії. Показано, що середні значення мікротвердості на поверхні та на сколах вирощених кристалів DAST розрізняються та складають 28,1 та 32,6 кгс/мм^2 відповідно. Встановлено кореляцію між значеннями мікротвердості і характером розподілу дислокацій у кристалах DAST.

Высококачественные кристаллы тозилата 4-*N*,*N*′-диметиламино-*N*-метил-4-стильбазола выращены на затравке из перенасыщенного раствора метанола методом контролируемого снижения температуры. Высокое структурное совершенство выращенных кристаллов подтверждено методом рентгенофазового анализа. Наличие функциональных групп, соответствующих кристаллам DAST идентифицировано с помощью инфракрасной спектроскопии. Показано, что средние значения микротвердости на поверхности и на сколе выращенных кристаллов DAST различаются и составляют 28,1 и 32,6 кгс/мм^2 соответственно. Установлена корреляция между значениями микротвердости и характером распределения дислокаций в кристаллах DAST.

1. Introduction

Organic nonlinear optical materials at present attract a lot of attention due to their potential applications in high-frequency electro-optical modulation, frequency conversion, generation and detection of broadband terahertz (THz) radiation [1, 2]. The structure of these materials consists of molecules with a developed system conjugated π-bonds, which are characterized by high polarizability. One of the most commercially successful organic nonlinear optical crystal is 4 *N*,*N*-dimetilamino-4′-*N*′-metilstilbazolium-tosylate (DAST) [3]. The coefficient of nonlinearity and the electrooptic coefficients DAST higher than those values in an inorganic crystal $LiNbO_3$, ten times and two times, respectively [4]. The high thermal stability of the organic crystal DAST (300°C) allows to use them in devices with high power switching signals [5].

Bulk single crystals of DAST are usually grown from a saturated solution by the traditional slow cooling technique, or by slow evaporation of the solvent [6].

However, difficulties still remain in crystal growth with sufficient quality for applications, such as optical and electro-optical sampling devices. The present article is focused on the high quality crystal growth of DAST and its characterization.

2. Experimental

4-*N*,*N*-dimethylamino-4′-*N*′-methyl-stilba zolium tosylate was synthesized at Division of Functional Materials Chemistry SSI "Institute for Single Crystals", NAS of Ukraine. The most common way to obtain DAST crystals of optical quality is growing by the temperature lowering method [6–9]. Methanol has been found to be the most suitable solvent for the growth of high-quality DAST crystals, because the solubility of DAST in methanol it is the highest among the most common organic solvents [10]. In order to determine the optimal concentration of a saturated solution the DAST solubility diagram was plotted (Fig. 1). Solubility was analyzed gravimetrically by evaporating the solvent at a constant temperature. It was also shown that the width of the metastable zone decreases with increasing temperature, which coincides with the results of [11]. Based on this data, we have chosen crystal growth temperature range from 43 to 30°C.

DAST crystals were grown onto a seed from supersaturated methanol solution by

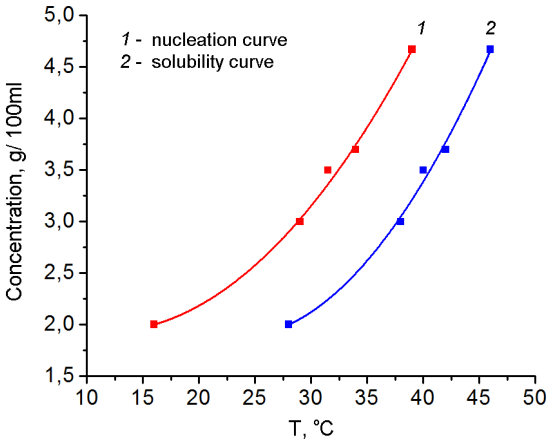

Fig. 1. Temperature dependences of the solubility of DAST in methanol.

controlled slow cooling technique. Constant supersaturation of the solution was ensured by continuous temperature decrease at a predetermined rate using contact thermometer and thermostat. The seed crystals measuring ~ 2×2 mm^2 were obtained by spontaneous nucleation. Seed with well-defined shape, without cracks and inclusions, were selected by means of a binocular microscope MC 50 (Austria).

DAST crystals were grown in a quartz crystallizer with a volume of 300 ml. The seeds were fixed attached to the crystal holder with silicone glue and placed in the growth volume. The solution was pumped into auxiliary volume at a temperature of 10°C above the equilibrium and kept at this temperature for a day. The solution was continuously stirred during this period. Then the growth apparatus cooled to a temperature 1°C above the saturation temperature of the solution, after which the solution from the auxiliary volume was pumped into the growth volume and slowly cooled to equilibrium temperature without mixing. Within 2 days, the temperature decrease was 10°C/day, then the temperature was lowered at a constant rate of 0.1–0.2°C/day until the temperature of the end of crystallization with stirring solution at a speed of 20 rpm with a reverse of 20 s. The average period crystal growing process was 30 days.

Powder XRD spectrum of the grown DAST crystals were recorded by the Diffractometer "Siemens D500" (with CuKα monochromatic radiation of wavelength λ = 1.54184 Å, Bragg-Brentano geometry, graphite monochromator) by step scan mode in the angle range $4° \le 2\theta \le 60°$, scan step 0.02°, accumulation time 5 sec. at every point.

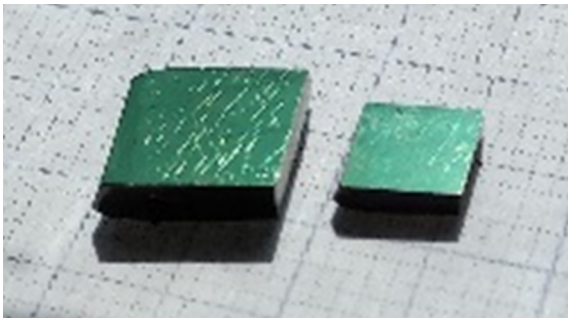

Fig. 2. Photo of grown DAST crystals.

The Fourier transform infrared (FTIR) spectra of the crystals were recorded using Spectrum One PerkinElmer spectrophotometer for the wavelength range 400–4000 cm^{-1} by KBr pellet (~ 0.16 wt % sample for all specimens) technique to confirm the functional groups. For the measurement of FTIR spectra of the sample we used crystalline powder of DAST.

3. Results and discussion

Fig. 2 present the photographs of the DAST crystal grown onto a seed from a supersaturated methanol solution using the slow cooling method. The crystals have the form of plates with the larger surface plane parallel to (001).

The surface of the investigated crystals has rounded steps with monoclinic symmetry corresponding to the symmetry of the face (001) (Fig. 3). The observed rounding of the microsteps seems to be due to the fact that the process of crystal growth onto a seed is realized under conditions of sufficiently large solution supersaturation and, accordingly, small interfacial tensions.

In Fig. 4 shows the diffractogram of the DAST sample refined by the Rietveld method. Appearance of sharp and strong peaks confirms the good crystallinity of the grown crystals. All samples were monophasic, their composition corresponded to the anhydrous salt $C_{16}H_{19}N_2 + C_7H_7O_3S^-$.

The lattice parameter values were calculated using the reflection angles of high intensity peaks corresponding to the *hkl* planes using the monoclinic crystallographic equation. The calculated lattice parameter are, space group C_c (point group m), a = 10.3553 Å, b = 11.3147 Å, c = 17.866 Å, β = 92.224°, V = 2093.35 $Å^3$, Z = 4. The lattice constant values are very much comparable with the literature data [12].

Functional groups of grown DAST crystals has been identified by FTIR spectroscopy. Fig. 5 shows the middle infrared (IR)

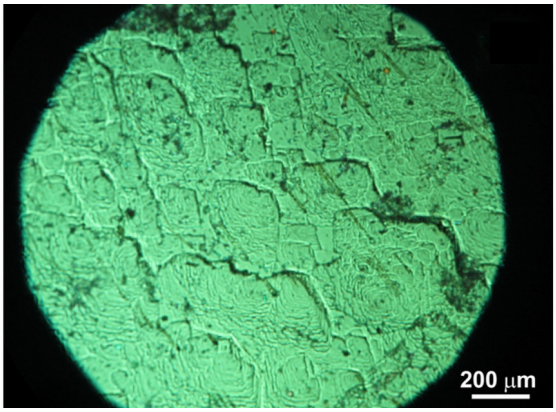

Fig. 3. The surface morphology of the grown DAST crystals.

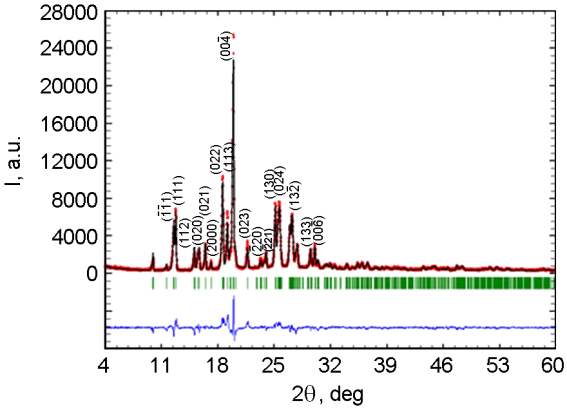

Fig. 4. Powder diffraction pattern of DAST. The experimentally obtained diffractogram is shown by the red curve, theoretically calculated by the Rietveld method — the black curve. The rows of vertical lines indicate the positions of the diffraction peaks. The difference between the experimental and calculated diffraction patterns is shown in the bottom curve.

spectrum of DAST samples. The peak at 1646 cm^{-1} is assigned to the stretching vibration C=C [13–15], a peak at 1580 cm^{-1} — to the aromatic rings vibration [11]. The band with a maximum at 1470 cm^{-1} corresponds to the asymmetric deformation vibration CH_3 (1475 cm^{-1} [14]). The band at 1438 cm^{-1} (in [14] shown the value 1436 cm^{-1}) is attributed to the ring stretching C=C. The peak at 1372 cm^{-1} is determined by CH_2 bending and C–N stretching [12], while peaks at 1372–1320 cm^{-1} (1370–1318 cm^{-1} in [14]) cause CH_3 deformation and C–N stretching.

Symmetric deformation of the CH_3 molecule appears at 1343 cm^{-1} [16]. The peaks at 1160 cm^{-1} and 1180 cm^{-1} (1163.59 cm^{-1} and 1180.47 cm^{-1} in [16]) are caused by the vibration of the S=O sulfonate groups. The

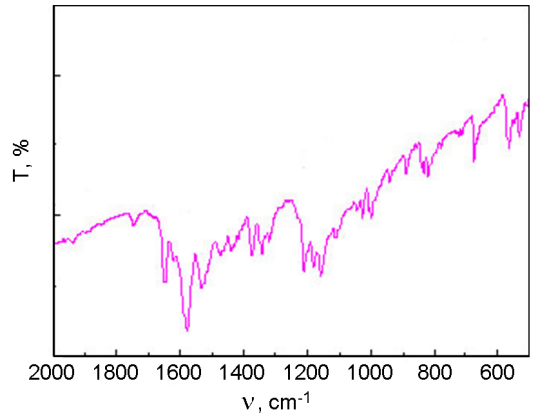

Fig. 5. FTIR spectrum of a DAST single crystal. Samples were prepared by KBr pellet technique.

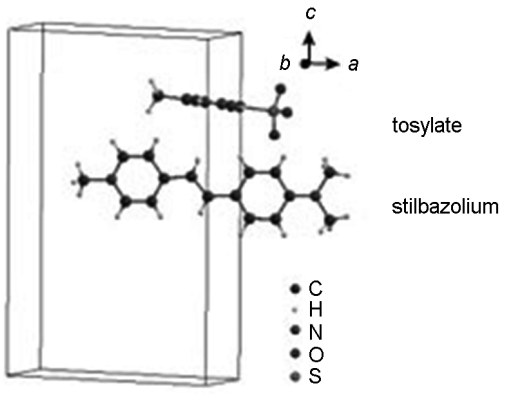

Fig. 6. Molecular arrangement of the DAST crystal.

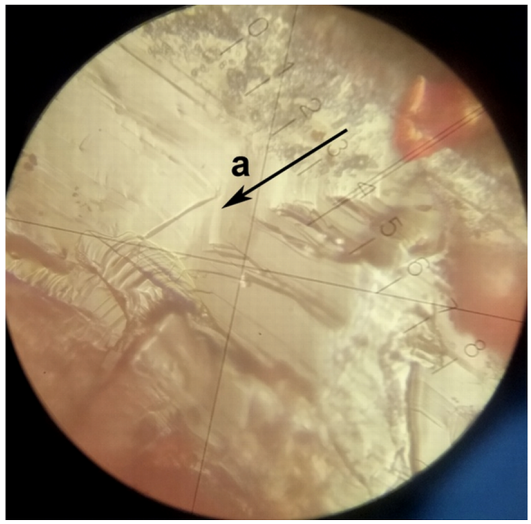

Fig. 7. Morphology of cleaved surface (001) of DAST crystal.

peaks at 1028 cm^{-1} in the IR spectrum are attributed to the stretching vibration of the C–H ring [14]. The peak at 889 cm^{-1} is explained by the stretching vibration of the C–N group [14]; out of plane C–H deformation vibrations are manifested in peaks at 833 cm^{-1} [14]. The aromatic hydrocarbon bend (C–H) is manifested in peaks at 834–818 cm^{-1} (834–818 cm^{-1} in [15]). Bending vibration of the C–C–C molecule was observed at 674 cm^{-1} (671 cm^{-1} in [14]).

The molecular packing of DAST is defined by stilbazolium, the cation, one of most efficient chromophores, and tosylate, the anion, which form the non-centrosymmetric crystal structure. DAST are multilayer molecular crystals. Their stilbazolium and tosylate molecules are arranged alternately parallel to the plane (001) in the form of ion pairs, thus providing balance of the electric charge of the crystal lattice (Fig. 6) [17].

It is known that an increase of the thickness of DAST crystals may diminish the efficiency of non-linear optical frequency conversion [18]. For large-size crystals such an effect is due to possible disorientation of the molecular layers. With an increase of the thickness of the crystal with sequential stratification, disorientation of the molecular layers rises. Under loading applied in the direction [001] DAST crystals were broken down parallel to the plane (001). Such loads exceeded the ones applied to the studied samples at mechanical treatment. The photograph present the pattern of the crystals surface split under the influence of external factors (Fig. 7). Step like patterns with monoclinic geometry are observed on the cleavage surface. This confirms the fact that the molecular layers in the bulk of the grown crystals are oriented along the plane (001).

The mechanical properties of the grown crystals were studied both on the surface and in the bulk of the sample. Shown in Fig. 8 are loading curves obtained on the surface of optically homogeneous crystals with a thickness of 3 mm (Fig. 8, curve *1*) and on the cleavaged surface of these crystals (Fig. 8, curve *2*). The measured microhardness increases rapidly at low indentation test loads, or for small indentation impression sizes. The curves show a load-dependent microhardness region at a low indenter load and a load-independent microhardness region at a high indenter load. The average values of microhardness obtained on the cleaved surface of the plate exceeded the ones for its surface and were equal to 32.6 and 28.1 kgf/mm2, respectively. The comparison was made for the values of microhardness in the load-independent hardness region.

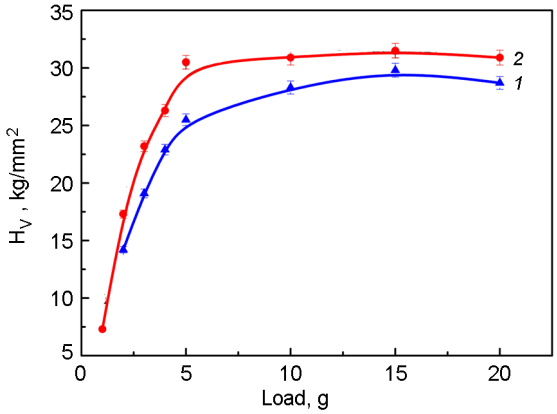

Fig. 8. Loading curves of the (001) plane of the DAST crystal: on the surface of the plate (*1*); on the surface of the cleaved plate (*2*).

Numerous dark etch pits with sharp peaks revealed on the surface of the grown crystals subjected to etching with metanol (Fig. 9,a). On the cleaved surface of this crystal, were observed only few etch pits (Fig. 9,b). Their morphology corresponds to the crystallographic symmetry of the examined plane and has the form of irregular parallelograms. Therefore, it may be assumed that the dark etch pits with peaks correspond to emergence of dislocations on the face in consideration. The dislocation density on the surface of the grown crystals essentially differed from the one in their bulk, and was equal to $5.7 \cdot 10^4$ cm^{-2} and $2.8 \cdot 10^2$ cm^{-2}, respectively. The dislocation density on the surface of a thick crystal exceeded the amount of linear defects in its bulk by more than two orders. This seems to be explained by relaxation of the interfacial stresses in the crystal induced by the bonding to the crystal holder.

The values of microhardness of the grown crystals correlates with the character of distribution of dislocations in them. The hardness of the surface layers of crystals, in which the dislocation density is relatively high, is 9–11 % lower than in the bulk perfect layers.

The mechanical strength is directly related to mobility of dislocations in the studied material. The increased dislocation density facilitates plasticity in the crystal. The increased dislocation density facilitates plasticity in the crystal. It may be assumed that the higher plasticity of the crystal grown onto a seed is due to the fact that the main deformation mechanism in it is not slipping which is limited in the dislocation forest, but climbing.

4. Conclusions

The solubility of DAST in methanol has been determined and bulk crystals of dimensions 8×6×3 mm^3 have been grown onto a seed from a supersaturated solution using the controlled slow cooling technique. Structural perfection was studied using the X-ray diffraction method. The functional groups of DAST were identified by FTIR studies. The average values of microhardness obtained on the surface and on the cleaved facet of the grown crystals are different and amount 28.1 and 32.6 kgf/mm^2, respectively. There is established a correlation between the values of microhardness and the character of distribution of dislocations in the crystals. The dislocation density

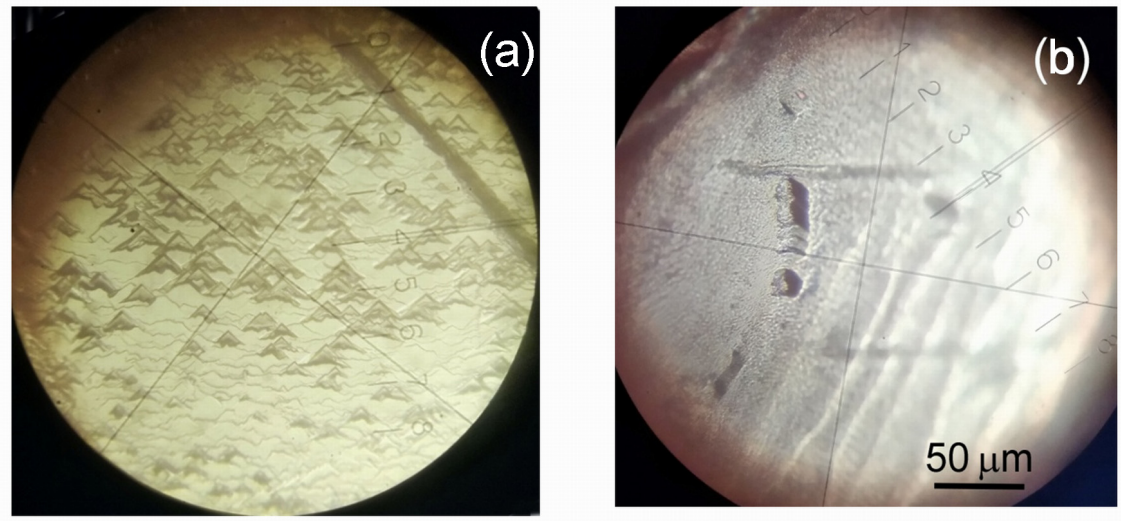

Fig. 9. Dislocation structure revealed by etching in methanol on the (001) face of the grown crystals: on the surface (a), in the volume (b).

on the surface of the crystal is essentially higher than in the bulk and equals $5.7 \cdot 10^4$ cm^{-2} and $2.8 \cdot 10^2$ cm^{-2}, respectively.

Acknowledgements. The authors gratefully acknowledge the National University of Mongolia for their financial support through the grant P2019-3741.

References

1. A.Barh, B.P.Pal, G.P.Agrawal et al., *IEEE J. Sel. Top. Quantum Electron.*, **22**, 365 (2016).
2. M.Jazbinsek, U.Pet, A.Abina et al., *Appl. Sci.*, **9**, 882 (2019).
3. K.Kumar, R.N.Ra, S.B.Rai, *Appl. Phys. B*, **96**, 85 (2009).
4. M.Jazbinsek, L.Mutter, P.Gunter, *IEEE J. Sel. Top. Quantum Electron.*, **14**, 1298 (2008).
5. I.Yu.Denisyuk, Yu.E.Burunkova, T.V.Smirnova, *J. Opt. Technol.*, **74**, 127 (2007).
6. B.Ruiz, M.Jazbinsek, P.Gunter, *Crystal Growth of DAST, Cryst. Growth Des.*, **8**, 4173 (2008).
7. K.Nagaoka, H.Adachi, S.Brahadeeswaran et al., *Jap. J. Appl. Phys.*, **43**, L261 (2004).
8. I.M.Pritula, A.V.Kosinova, D.A.Vorontsov et al., *J. Cryst. Growth.*, **335**, 26 (2012).
9. I.M.Pritula, V.I.Salo, M.I.Kolybaeva, *Inorg. Mater.*, **37**, 184 (2001).
10. Y.Mineno, T.Matsukawa, S.Ikeda et al., *Mol. Cryst. Liq. Cryst.*, **463**, 55/[337] (2007).
11. R.M.Kumar, D.R.Babu, G.Ravi et al., *J. Cryst. Growth.*, **250**, 113 (2003).
12. T.Bing, W.Shu-hua, F.Ke, *Cryst. Res. Technol.*, **49**, 943 (2014).
13. M.Manivannan, S.A.Martin Britto Dhas, M.Jose, *J. Cryst. Growth.*, **455**, 161 (2016).
14. K.Kumar, R.N.Rai, S.B.Rai, *Appl. Phys. B*, **96**, 85 (2009).
15. R.J.Vijay, N.Melikechi, T.Thomas et al., *Mater. Chem. and Phys.*, **132**, 610 (2012).
16. K.Jagannathan, S.Kalainathan, *Mater. Res. Bull.*, **42**, 1881 (2007)
17. H.Nanjo, K.Komatsu, T.Suzuki, *Thin Solid Films*, **464–465**, 425 (2004).
18. L.N.Asnis, Yu.E.Burunkova, A.V.Veniaminov et al., *J. Opt. Technol.*, **78**, 761 (2011).